Controllable Formation of Nanoscale Patterns on TiO_2 by Conductive-AFM Nanolithography

B. Garipcan,[†,‡] J. Winters,[‡] J. S. Atchison,[‡] M. D. Cathell,[‡] J. D. Schiffman,[‡] O. D. Leaffer,[‡] S. S. Nonnenmann,[‡] C. L. Schauer,[‡] E. Pişkin,[†] B. Nabet,[‡] and J. E. Spanier*[,‡]

Department of Chemical Engineering, Bioengineering Division, Hacettepe University, Beytepe, Ankara, 06800, Turkey, and Department of Materials Science and Engineering, Drexel University, Philadelphia Pennsylvania 19104

Received March 24, 2008. Revised Manuscript Received May 30, 2008

We report on the nanopatterning of double-bond-terminated silane (5-hexenyltrichlorosilane, HTCS) molecules on titania (TiO_2) using conductive atomic force microscopy (AFM). The influences of tip electrostatic potential and scanning velocity, relative humidity and of the repeated application of voltage on the topographic height, width, and hydrophilic and hydrophobic contrast of the resultant patterns were investigated. Tip voltage and tip velocity (υ) were applied between $-10\ V \le V_{tip} \le +10\ V$ and $100\ nm/s \le \upsilon \le 2\ \mu m/s$ during the lithography step(s), respectively. Average height and Lateral Force Mode (LFM) images of patterns were obtained with different values of ($-10\ V \le V_{tip} \le -7\ V$) and υ ($100\ nm/s \le \upsilon \le 2\ \mu m/s$). The average height of the patterns is seen to decrease for increasing υ and decreasing V_{tip} in both a single or repeated lithography step. No patterns were observed following a single or repeated lithography step for $-5\ V \le V_{tip} \le +10\ V$. This conductive lithography technique results in nanoscale physiochemical manipulations of the HTCS molecules that are manifested as controllable step heights ranging from ∼1−15 nm possessing different chemistries on the patterned and unpatterned areas. The use of conductive-AFM nanolithography for altering and manipulating double-bond-terminated molecules on TiO_2 surfaces suggests a range of applications, including selective immobilization and assembly of functionalized inorganic nanoparticles and biomolecules.

Introduction

The development of scanning proximal probe methods to produce nanoscaled features on inorganic surfaces in a controllable manner, and to introduce locally patterned chemical functionality, continues to attract significant interest. In part this is due to the prospects for the application of these methods to the fabrication of nanometer-scale devices and biological and chemical sensor arrays.[1–6] Several techniques have been developed to generate nanostructures utilizing an atomic force microscopy (AFM) tip.[7] Among these are dip-pen nanolithography,[8–11] ferroelectric nanolithography[12] and nanocatalysis.[13–15]

In conductive atomic force microscopy (c-AFM) nanolithography, a noble metal-coated AFM cantilever/tip is scanned along a preselected pattern in contact mode and with the application of a DC voltage. In the case of a negative applied bias and negatively charged tip, ambient water molecules are attracted to the tip, forming a water meniscus between the tip and the substrate. Under negative bias, electrons from the Fermi level of the metal-coated tip are injected into the water column whereupon they electrochemically reduce the water-forming hydroxyl ions (OH^-) and radicals ($H^\bullet$)[7] according to the following: $H_2O + e \rightarrow OH^- + H^\bullet$, and $H_2O + e \rightarrow OH^\bullet + H^+$. The $OH^\bullet$ consumption occurs via three pathways, namely (i) coupling with $H^\bullet$ radicals to produce water ($OH^\bullet + H^\bullet \rightarrow H_2O$), (ii) recombination to form hydrogen peroxide H_2O_2 molecules ($OH^\bullet + OH^\bullet \rightarrow H_2O_2$), and (iii) electrochemical reduction to hydroxyl ions at the tip−surface area ($e + OH^\bullet \rightarrow OH^-$).[16,17]

Conductive-AFM can alter the organic layer surface composition and topography corresponding to the patterned areas. There are several variables in c-AFM nanolithography that affect the physical topography and chemical changes of the nanopatterned areas, including applied voltage, tip velocity, humidity, tip conductivity and tip radius of curvature. In particular, the formation of nanoscale patterns of organic molecules on technologically important oxides (e.g., SiO_x-on-Si) using c-AFM is relevant for further development of chemical and biological sensors, and for molecular electronics involving DNA and protein arrays.[18,19] The surfaces of titania (TiO_2) are also of increasing

* To whom correspondence should be addressed. E-mail: spanier@drexel.edu.

† Hacettepe University.

‡ Drexel University.

(1) Basu, R.; Guisinger, N. P.; Greene, M. E.; Hersam, M. C. *Appl. Phys. Lett.* **2004**, *85*, 2619–2621.

(2) Demers, L. M.; Ginger, D. S.; Park, S. J.; Li, Z.; Chung, S. W.; Mirkin, C. A. *Science* **2002**, *296*, 1836–1838.

(3) Guisinger, N. P.; Greene, M. E.; Basu, R.; Baluch, A. S.; Hersam, M. C. *Nano Lett.* **2004**, *4*(1), 55–59.

(4) Kinser, R.; Schmitz, M. J.; Hersam, M. C. *Adv. Mater.* **2006**, *18*(11), 1377–1380.

(5) Liu, Z. M.; Yasseri, A. A.; Lindsey, J. S.; Bocian, D. F. *Science* **2003**, *302*, 1543–1545.

(6) Pavlovic, E.; Oscarsson, S.; Quist, A. P. *Nano Lett.* **2003**, *3*(6), 779–781.

(7) Hou, S.; Li, Z.; Li, Q.; Liu, Z. F. *Appl. Surf. Sci.* **2004**, *222*, 338–345.

(8) Hong, S.; Zhu, J.; Mirkin, C. A. *Langmuir* **2000**, *16*, 3927–3931.

(9) Piner, R. D.; Zhu, J.; Xu, F.; Hong, S.; Mirkin, C. A. *Science* **1999**, *283*, 661–663.

(10) Maynor, B. W.; Li, Y.; Liu, J. *Langmuir* **2001**, *17*, 2575–2578.

(11) Maynor, B. W.; Filocamo, S. F.; Grinstaff, M. W.; Liu, J. *J. Am. Chem. Soc.* **2002**, *124*, 522–523.

(12) Kalinin, S. V.; Bonnell, D. A.; Alvarez, T.; Lei, X.; Hu, Z.; Ferris, J. H.; Zhang, Q.; Dunn, S. A. *Nano Lett.* **2002**, *2*, 589–594.

(13) Mclntyre, B. J.; Salmeron, M.; Somorjai, G. A. *Science* **1994**, *265*, 1415–1418.

(14) Müller, W. T.; Klein, D. L.; Lee, T.; Clarke, J.; Mceuen, P. L.; Schultz, P. G. *Science* **1995**, *268*, 272–273.

(15) Schröder, U.; Mcintyre, B. J.; Salmeron, M.; Somorjai, G. A. *Surf. Sci.* **1995**, *33*, 1–333, 337−342.

(16) Lyuksyutov, S. F.; Paramanov, P. B.; Dolog, I.; Ralich, R. M. *Nanotech.* **2003**, *14*, 716–721.

(17) Park, J.; Lee, H. *Mater. Sci. Eng. C* **2004**, *24*, 311–314.

(18) Gu, J.; Yam, C. M.; Li, S.; Cai, C. *J. Am. Chem. Soc.* **2004**, *126*, 8098–8099.

10.1021/la800911x CCC: $40.75

Published on Web 07/23/2008

technological importance, in part due to the application of TiO_2 in solar cells,[20,21] optical waveguides,[22–24] gas sensors[25] and electrochromic displays,[26,27] and the impact of TiO_2 on medicine has been realized in orthopedic[28,29] and dental[30] applications because of its excellent biocompatibility.[31,32] Additionally, the immobilization of biomolecules onto TiO_2 substrates has been utilized in biorecognition templates,[33] bioseparation supports,[34,35] immuno-[36,37] and other biosensors,[38,39] and biochips.[40] Several organosilane molecules have been used to modify the surface of TiO_2 such as aminopropyltriethoxysilane (APTS),[41] (3,3,3-trifluoropropyl)trimethoxysilane (FPTS),[42] and octadecylsilanes with different headgroups ($C_{18}H_{37}SiH_3$,$C_{18}H_{37}Si(OCH_3)_3$, $C_{18}H_{37}SiCl_3$, and $C_{18}H_{37}Si(CH_3)_2Cl$)[43] for SAM formations and further modification with biological molecules.

Among organic layers used in c-AFM lithography, octadecyltrichlorosilane (OTS) is one of the more frequently used chlorosilane molecules. After performing c-AFM lithography, patterned areas of carboxyl (−COOH) groups formed by c-AFM were used for assembly of different nanostructures.[44–47] Molecules with different functional groups such as p-aminophenyltrimethoxy silane (APhS),[48] aminopropyltriethoxysilane,[17] ethylene glycol (OEG)-terminated monolayers,[18] and thiol-patterned surfaces[49] have been used as organic layers to investigate their chemical nature following c-AFM lithography, and to use their chemical functionalities for further applications. Also, monomers, precursors[50,51] and polymers[52] have been used as organic layers for c-AFM lithography.

Relatively little has been reported, however, on the formation of nanopatterns with the use of c-AFM nanolithography onto TiO_2 substrates. Kobayashi et al.[53] used c-AFM for the formation of nanoscale patterns of adsorbed oxygen molecules on Ti. In this study, c-AFM was used to nanopattern a TiO_2 surface modified by a double-bond containing silane molecule [5-hexenyltrichlorosilane (HTCS)]. HTCS was selected as the organic layer to investigate both its chemical and physical evolution under different conditions and at different stages of c-AFM lithography. The effects on pattern topography and hydrophilicity/hydrophobicity of applied voltage, tip velocity, relative humidity and repeated application of voltage once to the patterning areas were investigated. Conductive lithography results in nanoscale physiochemical manipulation of the molecules manifested as controllable step heights ranging from ∼1−15 nm, and with different chemistries on the patterned and nonpatterned areas. The use of c-AFM nanolithography for altering and manipulating double-bond-terminated molecules on TiO_2 surface as presented herein may expand applications of c-AFM nanolithography, including the selective immobilization and/or assembly of functionalized inorganic nanoparticles and/or biomolecules.

Results and Discussion

The experimental procedures are illustrated schematically in Figure 1a−c, and details are provided in the Methods section. Shown in Figure 2a−f are representative height profiles and corresponding lateral force microscopy (LFM) images for selected values of tip voltage $-10\ \text{V} \le V_{tip} \le +10\ \text{V}$ and tip velocity v during the lithography step(s) $100\ \text{nm/s} \le v \le 2\ \mu\text{m/s}$, revealing that the average height of the patterns are seen to decrease for increasing v. Specifically, as seen in Figure 2e for $V_{tip} = -10$ V and selected values indicated along the first "writing" segment (see Figure 1c), the average height of the patterned lines decreased from 10.31 ± 2.80 nm to 3.50 ± 0.72 nm. Moreover, for $V_{tip} = -9$ V (Figure 2c) and $V_{tip} = -8$ V (not shown) applied along the first written segment with $100\ \text{nm/s} \le v \le 2\ \mu\text{m/s}$, the heights of the patterns were also seen to decrease, from 8.77 ± 0.71 to 2.72 ± 0.26 nm and 6.86 ± 1.18 to 1.58 ± 0.30 nm, respectively. When c-AFM nanolithography was performed using a *second* "writing" step along each segment and at the same voltages (as denoted schematically in Figure 1c in the lower part of the scanned areas), qualitatively similar behavior was observed. The line heights following two successive writing steps decreased for increasing values of v ($100\ \text{nm/s} \le v \le 2\ \mu\text{m/s}$): from 12.22 ± 1.01 to 5.07 ± 0.98 nm for $V_{tip} = -10$ V, from 9.61 ± 0.66 nm to 3.62 ± 0.21 nm for $V_{tip} = -9$ V, and from 7.18 ± 0.23 nm to 2.47 ± 0.47 nm for $V_{tip} = -8$ V. Although no height difference following the single writing step was discerned for $V_{tip} = -7$ V, a height change for $V_{tip} = -7$ V, from 4.63 ± 0.24 nm to 1.05 ± 0.53 nm, was observed following the second writing step at $V_{tip} = -7$ V (Figure 2a). In addition, for $V_{tip} = -6$ V, a height change (1.5 nm) was observed only using the smallest selected value of $v = 100$ nm/s following two successive scans. In Tables 1 and 2, we summarize the results of the effects of applied voltage, and single and multiple writing on pattern height and width. No patterns were observed following a single or repeated lithography step for $-5\ \text{V} \le V_{tip} \le +10\ \text{V}$. Additionally, no changes in the surface topography or chemistry could be discerned.

We also repeated the lithography by applying the highest and the lowest voltages (−10 V and - 7 V) on a bare TiO_2 surface.

(19) Zhao, Z.; Banerjee, I. A.; Matsui, H. *J. Am. Chem. Soc.* **2005**, *127*, 8930–8931.
(20) O'Regan, B.; Gratzel, M. *Nature* **1991**, *353*, 737–740.
(21) Barbe', C. J.; Arendse, F.; Comte, P.; Jirousek, M.; Lenzmann, F.; Shklover, V.; Gratzel, M. *J. Am. Ceram. Soc.* **1997**, *80*, 3157–3288.
(22) Yoshida, M.; Prasad, P. N. *Chem. Mater.* **1996**, *8*, 235–241.
(23) Que, W.; Zhou, Y.; Lam, Y. L.; Kam, C. H. *Appl. Phys. A* **2001**, *73*, 171–176.
(24) Que, W.; Kam, C. H. *Opt. Eng.* **2002**, *41*, 1733–1737.
(25) Arakawa, S.; Mogi, K.; Kikuta, K.; Yogo, T.; Hirano, S. *J. Am. Ceram. Soc.* **1999**, *82*, 225–228.
(26) Ohzuku, T.; Hirai, T. *Electrochim. Acta* **1982**, *27*, 1263–1266.
(27) Livage, J. *Mater. Res. Soc. Symp. Proc.* **1986**, *73*, 717–722.
(28) Milella, E.; Cosentino, F.; Licciulli, A.; Massaro, C. *Biomaterials* **2001**, *22*, 1425–1431.
(29) Oh, S. H.; Finones, R. R.; Daraio, C.; Chen, L. H.; Jin, S. *Biomaterials* **2005**, *26*, 4938–4943.
(30) Rupp, F.; Geis-Gerstorfer, J.; Geckeler, K. E. *Adv. Mater.* **1996**, *8*, 254–257.
(31) Lee, S. H.; Kim, H. W.; Lee, E. J.; Li, L. H.; Kim, H. *J. Biomater. Appl.* **2006**, *20*, 195–208.
(32) Wu, J. M.; Hayakawa, S.; Tsuru, K.; Osaka, A. *Thin Solid Films* **2002**, *414*, 283–288.
(33) Huang, J. G.; Ichinose, I.; Kunitake, T. *Angew. Chem., Int. Ed.* **2006**, *45*, 1–5.
(34) Andre, L. M. P.; Flávia, C.; Silvio, L. P. D.; Ines, J; Yoshitaka, G.; Jose, A. R. R.; Paulo, J. S. M.; Gilson, P. M.; Anita, J. M. *J. Mol. Catal. B: Enzym.* **2002**, *19−20*, 327–334.
(35) Chen, Y.; Yi, Y.; Brennan, J. D.; Brook, M. A. *Chem. Mater.* **2006**, *18*, 5326–5335.
(36) Stamm, C.; Lukosz, W. *Sens. Actuators, B* **1996**, *31*, 203–207.
(37) Clerc, D.; Lukosz, W. *Sens. Actuators, B* **1997**, *40*, 53–58.
(38) Zhang, Y.; He, P. L.; Hu, N. F *Electrochim. Acta* **2004**, *49*, 1981–1988.
(39) Andre, B.; Hans, R. B. *Eur. J. Biochem.* **1995**, *230*, 416–423.
(40) Li, Q. W.; Luo, G. A.; Feng, J.; Zhou, Q.; Zhang, L.; Zhu, Y. F. *Electroanalysis* **2001**, *13*, 413–416.
(41) Ye, L.; Pelton, R.; Brook, M. A. *Langmuir* **2007**, *23*, 5630–5637.
(42) Gamble, L.; Henderson, M. A.; Campbell, C. T. *J. Phys. Chem. B* **1998**, *102*, 4536–4543.
(43) Helmy, R.; Fadeev, A. Y. *Langmuir* **2002**, *18*, 8924–8928.
(44) Hoeppener, S.; Maoz, R.; Cohen, S. R.; Chi, L. F.; Fuchs, H.; Sagiv, J. *Adv. Mater.* **2002**, *14*(15), 1036–1041.
(45) Maoz, R.; Cohen, S. R.; Sagiv, J. *Adv. Mater.* **1999**, *11*(1), 55–61.
(46) Maoz, R.; Frydman, E.; Cohen, S. R.; Sagiv, J. *Adv. Mater.* **2000**, *12*, 725–731.
(47) Wouters, D.; Schubert, U. S. *Langmuir* **2003**, *19*, 9033–9038.
(48) Saito, N.; Maeda, N.; Sugimura, H.; Takai, O. *Langmuir* **2004**, *20*, 5182–5184.
(49) Fresco, Z. M.; Fréchet, J. M. J. *J. Am. Chem. Soc.* **2005**, *127*, 8302–8303.
(50) Baba, A.; Locklin, J.; Xu, R.; Advincula, R. *J. Phys. Chem. B* **2006**, *110*, 42–45.
(51) Jegadesan, S.; Sindhu, S.; Advincula, R. C.; Valiyaveettil, S. *Langmuir* **2006**, *22*, 780–786.
(52) Martin, C.; Rius, G.; Borrisé, X.; Perez-Murano, F. *Nanotech.* **2005**, *16*, 1016–1022.
(53) Kobayashi, K.; Tomita, Y.; Yoshida, S. *Nano Lett.* **2002**, *2*, 925–927.

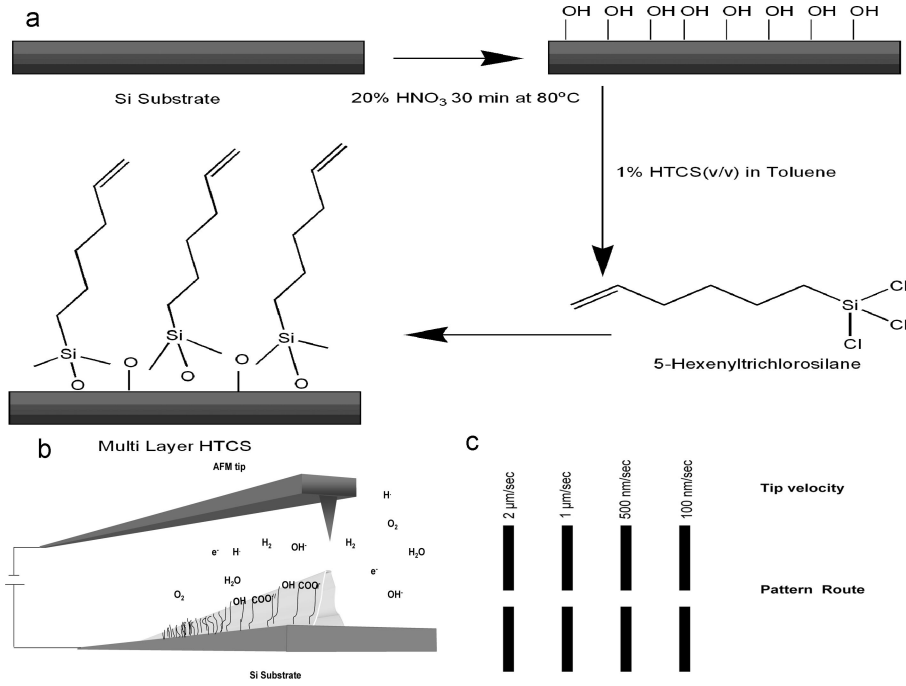

Figure 1. Schematic illustration of experimental procedures; (a), TiO_2 surface modification with 5-hexenyltrichlorosilane (HTCS); (b), possible chemical environment during c-AFM nanolithography; and (c), lithography scheme using predesigned patterns, with voltage applied to the tip using a different tip velocity υ (100 nm/s $\leq \upsilon \leq$ 2 μm/s) for one writing lithographic step (upper segments), and that for two lithographic writing steps, each pair along an identical path.

For the TiO_2 surface, patterns were also formed when -10 V and - 7 V was applied by performing a second lithographic writing step following the single lithographic writing step using a tip velocity υ (100 nm/s) to the bare TiO_2 surface (the relative humidity was between 65−69%). We observe average heights of the patterns to be 1.96 ± 0.3 nm and 3.17 ± 0.2 nm for -10 and -7 V, respectively (Supporting Information, Figure s1), significantly smaller than that for the same conditions with the HTCS-modified TiO_2 surface. (For the same conditions, the average heights of the patterns are 12.22 ± 1.01 nm and 4.63 ± 0.24 nm for -10 and -7 V (Table 1) on the HTCS-modified TiO_2 surface.) We estimate, based on variable-angle and spectroscopic ellipsometry, the average thickness of the HTCS layer to be ∼6 nm. It is likely that the HTCS layer inhibits the diffusion of oxygen radicals into the TiO_2 film, thereby suppressing oxidation-induced pattern formation. In Figure 3a and b, the average height differences (relative to the background values) following (a) a single, and alternatively, (b) following a second c-AFM lithography step at selected values of V_{tip}, and υ are presented, summarizing the effects of voltage, tip velocity, and successive lithography steps.

Shown in Figure 2b, d, and f are LFM images of patterns obtained with different values of V_{tip} (-10 V $\leq V_{tip} \leq -7$ V) and υ (100 nm/s $\leq \upsilon \leq$ 2 μm/s). The contrast mechanism in LFM is attributed to local maxima in the surface free energy (as compared with surrounding areas) that result from increasing the polarity of the functionalized regions. This condition produces a stronger attractive interaction between the polar AFM tip as it scans the surface, which is manifested as an increase in the frictional force.[54]

As seen from Figure 2f, the application of $V_{tip} = -10$V at υ = 100 nm/s results in patterns which are observed to be hydrophobic following both the first and second lithography steps. However, for progressively larger values of υ, the patterns exhibit a more hydrophilic character. This may be explained in terms of a polymerization and/or cross-linking of the vinyl groups of the HTCS molecules at the nanopatterned areas. We suggest that a competition between hydroxyl and hydrogen radicals exists, such that at larger negative voltages and low tip velocities, high hydrogen radical introduction to the nanopatterned area results with polymerization and/or cross-linking, exhibiting more hydrophobic characteristics. From the LFM images with $V_{tip} = -9$V, hydrophobic areas are localized near the center of the patterned lines, and hydrophilic areas are located at the outer areas of the patterned lines (Figure 2d). The concomitant decrease in the LFM contrast (expressed in ΔmV, not shown) for low (100 nm/s) to high (2 μm/s) tip velocities suggests that more hydrophilic atoms or molecules are introduced to the nanopatterned areas. Among the values of V_{tip} used, the largest change (in mV) and therefore the highest hydrophilic group introduction was obtained with $V_{tip} = -8$V(not shown). When, $V_{tip} = -7$V during the first writing pass, patterns were not discernible in either topographic height (Figure 2a) or LFM (Figure 2b) signals.

Lyuksyutov, et al.[16] suggested that water acts as a two-electrode nanocell between the tip and the surface during the application of a voltage to the AFM tip in the presence of humidity, creating electrons, protons and free radicals (OH•). Introduction of more electronegative oxygen atoms (from OH molecules or O^-) to the structure of the pattern causes an increase in the polarity of the patterned area, making the patterned area more negatively charged. With $V_{tip} = -10$V, the highest topographic change was observed (for all values of υ used), and this change was accompanied by a less hydrophilic change on the patterned areas, owing to strong interactions with negatively charged tip. As the hydrophilicity was increased (for smaller negative voltages $V_{tip} = -9$V and -8V), the largest hydrophilic change was observed at $V_{tip} = -8$V (corresponding to the introduction of more electronegative molecules), resulting in less interaction with the tip, leading to smaller final pattern heights. With $V_{tip} = -7$V water decomposi-

(54) Sun, S.; Montague, M.; Critchley, K.; Chen, M. S.; Dressick, W. J.; Evans, S. D.; Leggett, G. J. *Nano Lett.* **2006**, *6*(1), 29–33.

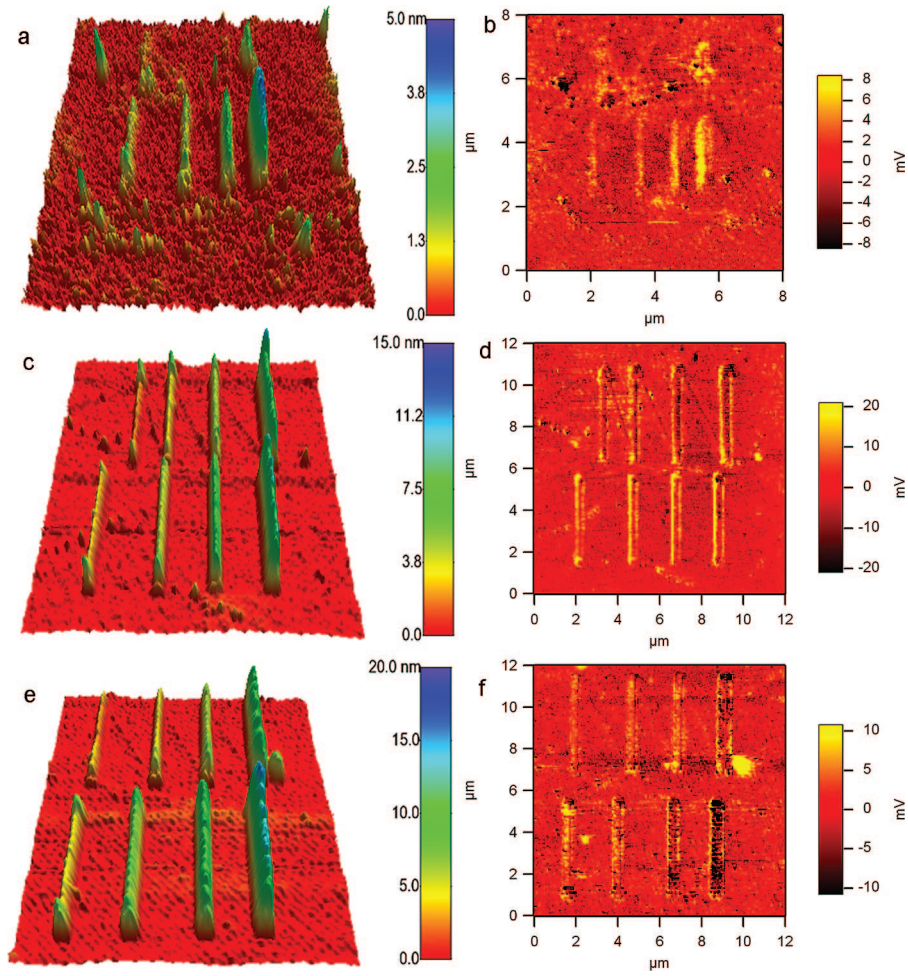

Figure 2. Effects of applied voltage V_{tip} and tip velocity v on pattern topography and hydrophilicity; (a) topographic height, and (b) corresponding lateral force microscopy (LFM) images for $V_{tip} = -7$V and RH = 64%.; (c) height and (d) corresponding LFM images for $V_{tip} = -9$V and RH = 67%; and (e) height and (f) corresponding LFM images for $V_{tip} = -10$V and at a relative humidity (RH) of 70%. For each value of V_{tip} selected values of tip velocity were used as described in the main text, and the lower patterns were imaged following an additional lithography patterning step as described in the main text and in Figure 1c. The area shown for each topographic height image corresponds to the area shown in the corresponding LFM image.

Table 1. Effects of Applied Voltage, Single and Multiple Writing on Pattern Height

	first writing				second writing			
	tip velocity (v)				tip velocity (v)			
applied voltage (V)	100 nm/sec	500 nm/sec	1 μm/sec	2 μm/sec	100 nm/sec	500 nm/sec	1 μm/sec	2 μm/sec
	height (nm)				height (nm)			
−10	10.31± 2.80	6.78 ± 0.56	5.48 ± 0.39	3.50 ± 0.72	12.22 ± 1.01	9.18 ± 0.42	6.97 ± 0.38	5.07 ± 0.98
−9	8.77 ± 0.71	5.34 ± 0.38	4.03 ± 0.28	2.72 ± 0.26	9.61 ± 0.66	7.03 ± 0.23	5.21 ± 0.57	3.62 ± 0.21
−8	6.86 ± 1.18	3.53 ± 0.32	2.28 ± 0.54	1.58 ± 0.30	7.18 ± 0.23	4.73 ± 0.71	3.56 ± 0.50	2.47 ± 0.47
−7	0.93 ± 0.56	0.37 ± 0.28	0.30 ± 0.21	0.42 ± 0.34	4.63 ± 0.24	3.14 ± 0.48	1.94 ± 0.53	1.05 ± 0.53

Table 2. Effect of Applied Voltage on Pattern Width

applied voltage (V)	width (nm)
−10	1004.17 ± 128.22
−9	920.83 ± 123.80
−8	815.10 ± 64.13
−7	772.29 ± 68.33

tion into hydroxyl ions (OH^-) and radicals ($H^\bullet$) was not sufficiently negative enough to change the chemical composition of the patterns, and this resulted in the lowest height profile and hydrophilic change of all values of applied voltage.

Are the OH molecules solely responsible for the apparent hydrophilicity and/or topology of the observed patterns? Different studies have shown different answers to this question: for example, Sagiv et al.[44] used NTS [18-nonadecenyltrichlorosilane, $(CH_2{=}CH{-}(CH_2)_{17}{-}SiCl_3)$] for the modification of Si and after performing AFM nanolithography, the authors demonstrated by using Brewster-angle FTIR spectrophotometer, conversion of top vinyl groups to carboxylic acid groups (NTS_{ox}). On the other hand, Pignatore et al.[55] used 1-octedecene-modified hydrogenated silicon surfaces for AFM nanolithography, and showed using time-of-flight secondary ion mass spectroscopy, the presence of C_xH_yO peaks, but no evidence of carboxylic acid groups after lithography.

We believe both OH and COOH groups can be formed during our nanolithography procedure, causing both topological and

(55) Pignataro, B.; Licciardello, A.; Cataldo, S.; Marletta, G. *Mater. Sci. Eng. C* **2003**, *23*, 7–12.

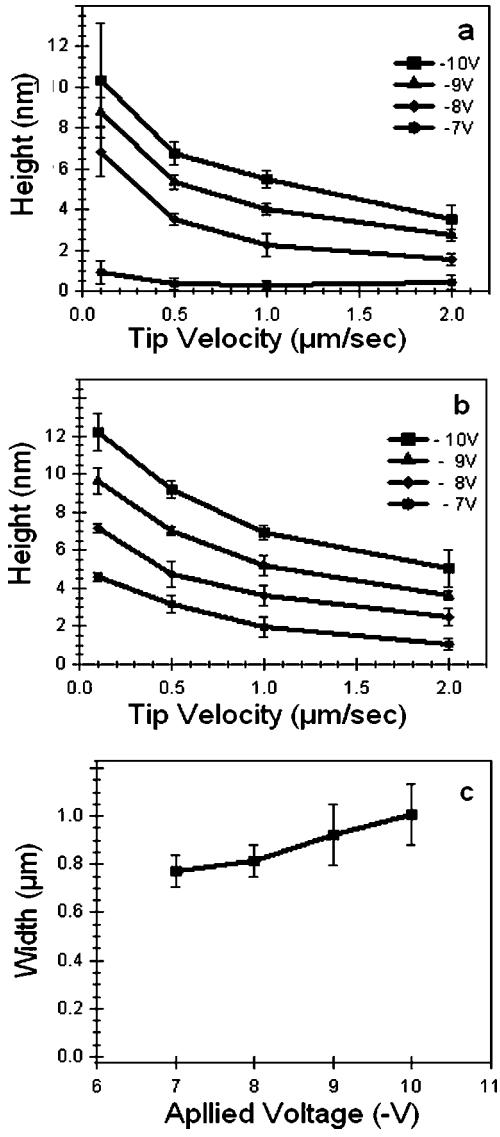

Figure 3. Effect of applied voltage and tip velocity on pattern height and width; (a) average height change, demonstrating its dependence on applied voltage and tip velocity following a single lithographic writing step; (b) average height change following a second lithographic writing step along the same path as the first, demonstrating dependence on applied voltage and tip velocity; and (c) average widths of patterns following second lithographic writing step.

chemical changes on the patterned areas. The environment during the lithography depends on several parameters, including applied voltage, tip velocity, tip type, tip diameter, humidity as well as the chemical behavior of the patterned molecules. Thus, the reactivity of hydroxyl, hydrogen, and oxygen radicals would likely be different and result in functionalization by a different chemical group (hydroxyl and carboxyl) on the patterned areas.

The effect of applied voltage on pattern width was also studied. The produced patterns are seen to be narrower for progressively smaller negative voltages following the second writing step (from $V_{tip} = -10$ to -7 V) at constant tip velocity (100 nm/s). Figure 3c shows the dependence of the line width on applied voltage.[56] As seen from Figure 3a−c the height and the width of the patterns decreases for progressively smaller negative values of applied voltage (-10 V $\leq V_{tip} \leq -7$ V). This may be due to the fact that in some polymer films such as poly(*N*-vinylcarbazole) (PVK)[50] as well as in our HTCS film, the side group monomer is tethered to a polymer backbone and therefore governed by the viscoelastic nature of the polymer where the effect of local Joule heating has been shown to be dramatic under higher applied electric fields bias.,[51 57] In addition, we observe that relative humidity (RH) influences pattern height and width (Figure 4). With $V_{tip} = -10$ V and $v = 100$ nm/s at a RH of 39%, 3.10 ± 0.63 nm-high patterns were formed. At the same applied voltage and tip velocity, when RH was 59%, patterns were formed with a height profile of 9.23 ± 1.64 nm. At high RH values, higher concentration of hydroxyl ions (OH^-) and/or radicals ($H^\bullet$) formed from water molecules and resulted in higher height profiles. In terms of pattern width, no significant difference was observed. Below 30% RH, no patterns were formed.

In summary, the formation of nanoscaled patterns of HTCS on titania (TiO_2) by c-AFM has been reported. The effects of tip voltage, tip velocity, and humidity were investigated. On the same substrate, nanoscale height features possessing different chemical properties were formed based on control of tip voltage, tip velocity and humidity. The results presented herein suggest applications of c-AFM nanolithography to titania and other transition-metal oxide films. Such patterned surfaces resulting in selectable nanoscale height, hydrophobic/hydrophilic character, and with double-bonded molecules may find application in the chemically selective immobilization of nanostructures, biological molecules, and cells.

Methods

The experimental procedures are illustrated schematically in Figure 1a−c. Briefly, HTCS [5-hexenyltrichlorosilane, Sigma Aldrich (95%)] was used without further purification. Si(100) substrates possessing TiO_2 thin-film coatings (University Wafer) were cleaned in ethanol, acetone, deionized (DI) H_2O and dried in N_2 gas. The substrate was then incubated in 20% HNO_3 solution for 30 min. at 80 °C to generate a Ti-OH terminated surface. The Ti-OH terminated substrate was washed three times with DI H_2O water, dried in N_2 gas, and then immersed in solution of HTCS (1%, v/v) in toluene for 30 min. (Figure 1a). Afterward, the functionalized substrate was cleaned with toluene and acetone. Finally, the substrate was cleaned again in toluene using an ultrasonic bath for 2 min in order to remove physisorbed species. No optimization studies were made to correlate film thickness, such as HTCS concentration and immersion time. All measurements were performed with a scanning probe microscope (Asylum Research MFP-3D, Santa Barbara CA) using Pt-coated Si cantilevers (Olympus AC240TM, force constant of ∼2 N/m) operating in contact mode for patterning at atmosphere in an enclosed (acoustic isolation) chamber at selected values of humidity (30−70%), and temperature (21−25 °C). The effects on surface topography and hydrophobicity/hydrophilicity of the patterned areas due to applied voltage to the tip, tip velocity, humidity and application of voltage once or twice to the patterning regions were investigated (Figure 1b and c).

Conductive-AFM nanolithography was performed by applying to the cantilever tip a voltage V_{tip} while scanning linear patterns in contact mode, and the "writing" directions were parallel to the AFM cantilever axis. Selected values of tip voltage V_{tip} −10 V $\leq V_{tip}$ +10 V were applied, and the relative humidity and temperature were recorded and ranged from 30−70% and 21−25 °C, respectively (APC, Environmental Monitoring Unit Model No. AP9319, RI, USA). Following contact-mode conductive nanolithography, contact-mode imaging with an identical voltage

(56) Park, C. H.; Bae, S.; Lee, H. *Colloids Surf., A* **2006**, *284−285*, 552–555.

(57) Lyuksyutov, S. F.; Vaia, R. A.; Paramonov, P. B.; Juhl, S.; Waterhouse, L.; Ralich, R. M.; Sigalov, G.; Sancaktar, E. *Nat. Mater.* **2003**, *2*, 468–472.

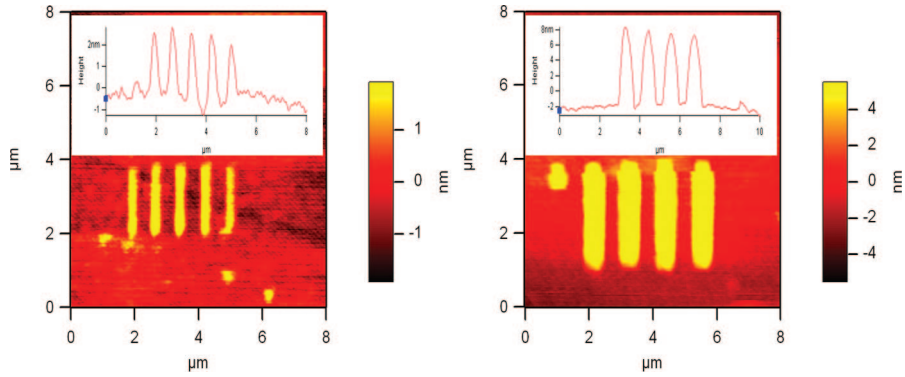

Figure 4. Effect of relative humidity on pattern topography; left, height image at $V_{tip} = -10$V, RH = 39%, and $\upsilon = 100$ nm/s; right, height image at $V_{tip} = -10$V, RH = 59%, and $\upsilon = 100$ nm/s, with representative height traces shown for each.

(deflection) feedback set point was performed in which the normal and lateral force microscopy (LFM) signals were collected simultaneously (with the fast scan axis perpendicular to both the cantilever's long axis as well as the direction of the lithographic pattern-writing) in order to obtain spatially correlated maps of local topography and frictional force on the HTCS-modified TiO_2 substrates. The topographic height and width values reported here were obtained by selecting and analyzing 15 line height and width profiles perpendicular to the patterns at locations selected randomly along each line pattern within each topographic height image. Heights and widths reported are average values ± a standard deviation obtained from least-mean-squares fitting of the distributions by a Gaussian (not shown).

Acknowledgment. J.S. acknowledges support from the U.S. Army Research Office (W911NF-04-100308), and from the Nano-Bio Interface Center, an NSF-NSEC program (DMR-0425780)) at the University of Pennsylvania and Drexel. B.N. and J.S. also acknowledge partial support from the National Science Foundation (ECCS-0707716). B.G. is supported by a TUBITAK-NATO A2 scholarship from Turkey, and J.W. was supported under an NSF Research Experiences for Undergraduates (REU) program at Drexel (EEC-0552711).

Supporting Information Available: Conductive-AFM nanolithography was performed on a bare, HTCS-free TiO_2 surface at selected applied voltages. This material is available free of charge via the Internet at http://pubs.acs.org.

LA800911X